

Deep cryogenic treatment of AA7050: tensile response and corrosion susceptibility

R. Gerosa¹ · D. Panzeri¹ · B. Rivolta¹ · A. Casaroli¹

Received: 4 November 2022 / Accepted: 6 February 2023

Published online: 12 February 2023

© The Author(s) 2023 [OPEN](#)

Abstract

Cryogenic treatments represent an innovative technology developed with the aim of improving the performance of metallic alloys. The beneficial effects on steels are well documented in the literature, whereas their influence on other materials, such as aluminum alloys, is still not completely clarified. Even if the scientific literature reports conflicting data and conclusions, the industrial applications of such treatments are constantly growing. In the present experimental work, the mechanical and corrosion properties of a high-performance 7050 aluminum alloy plate were studied after cryogenic treatment at $-196\text{ }^{\circ}\text{C}$ in liquid nitrogen. Tensile tests were performed on heat-treated samples, and intergranular corrosion tests were carried out on prismatic samples, according to ASTM G110-92 standard. The specimens were exposed to the corrosive environment and the effect of intergranular corrosion was measured by quantitative analysis using light-optical microscopy (LOM). Whereas trifling variation was observed in the mechanical resistance and plastic behavior, the corrosion tests showed a benefic effect of the cryogenic treatment. The microstructure was investigated by FEG-SEM analysis, revealing a different distribution of precipitates near the grain boundaries, which was able to reduce the electrochemical potential difference among these regions and the center-grain.

Keywords Cryogenic treatment · Aluminum alloys · Mechanical resistance · Corrosion resistance · Metallography

1 Introduction

Aluminum alloys are one of the most important materials in engineering structures. Among them, the so-called 7xxx series, based on the Al–Zn–Mg (–Cu) system, is characterized by the highest mechanical strength. They are widely used in high-performance structural, aerospace and transportation applications. Together with the chemical composition and the fabrication process, their properties are significantly influenced by the heat-treating procedure, which involve three basic steps: high-temperature solubilization, water quenching and natural or artificial aging. In the precipitation response, the peak hardening is obtained at precise time–temperature conditions [1–5]. Depending on the chemical composition, in standard heat treatments [1, 2], the precipitation sequence can be very complicated and can involve many stable and/or metastable compounds [1, 2].

In recent years, a further and innovative possibility to improve the service performance of metallic alloys has been identified in the cryogenic treatment (CT). It consists of a gradual cooling of the material until the defined temperature, holding it for a given time and then progressively returning it to room temperature. The aim is to induce a microscopic modification of the material resulting in improved mechanical, wear and corrosion resistance [6–8].

✉ B. Rivolta, barbara.rivolta@polimi.it | ¹Dipartimento di Meccanica, Politecnico di Milano, Via la Masa 34, 20156 Milan, Italy.



The first practical applications of purposely executed CTs were developed starting from the second half of the twentieth century [9]. It was only during the World War II that the cryogenic processing of tooling equipment was investigated as part of the researches conducted at the Watertown Arsenal (Massachusetts, USA). The first cryogenic processing techniques consisted in dipping the tools in a bath of liquid nitrogen for a brief period of time and in letting the components warm up before placing them in service [9]. Most of the treated tools fractured immediately upon use, as a result of the propagation of micro-cracks nucleated for thermal shocks. The tools were characterized by higher hardness and strength [9]. The outcomes of those processes were so promising that in the following years several efforts were made to develop more sophisticated apparatuses, with the aim of minimizing the thermal shocks. In late '60 s, Ed Busch introduced an innovative cryo-chamber design containing a nebulization system: the direct contact between the workpieces and the liquid nitrogen was avoided, thus minimizing the thermal shocks. [9]. Busch's idea was later refined by Peter Paulin, who added a temperature feedback control system to the cryo chamber in order to reach controlled heating and cooling rates. The introduction of innovative apparatuses regulated by computers greatly increased the efficacy of CTS in creating more favourable residual stresses in the samples [9–11]. During the Cold War the development of the space programs raised the need to investigate the behaviour of different materials at extremely low temperatures, as well as the effects that the exposure to cryogenic temperatures had on their characteristics. As a result, many different materials other than tool steels were progressively investigated, including copper and aluminium alloys, as well as several polymers and ceramics [9].

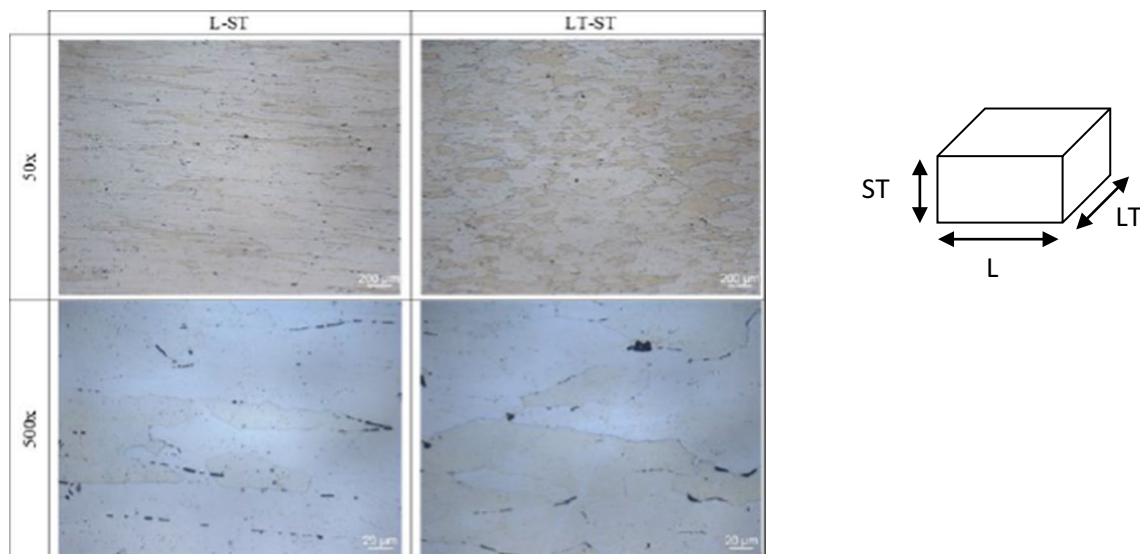
The subject has become more interesting for research in the last five years, due to the pressure of general public and science as a response to the climate impact, natural resources and development of various industries. In high-alloyed steels and cast irons, several authors have demonstrated an increase in the mechanical, electrical and corrosion response after CT [9, 10, 12], linked to microstructural changes promoting the conversion of retained austenite into martensite and inducing carbide precipitation [11–23]. This supplementary treatment has also been used to improve some properties in other non-ferrous alloys, such as magnesium, copper and titanium [24–26]. The adoption of this heat treatment to increase the mechanical properties of aluminium alloys is quite recent [27, 28], but the real influence of CT has not yet been clarified. Several studies were found in the technical literature [8, 29–44], but the obtained results are often contradictory and not always justified by microstructural modifications.

Steier et al. [6] studied the effects of DCT on the microstructure and mechanical resistance of a 6XXX aluminium alloy. They found a slight reduction in hardness and a significant improvement in wear resistance (+27%). Wen-da Zhang et al. [39] studied the response of a recycled 3XXX aluminium alloy to different sequences of homogenization and DCTs. They found that, when only subjected to DCT, the alloy showed a 20% increase in ultimate tensile strength, even though maximum elongation was reduced. The effects of multiple cryogenic treatments on the 2XXX aluminium alloy were investigated by Junjie Wang et al. [7]. The mechanical properties improved after a single DCT carried out on the as-quenched alloy, while the results were not so positive if DCT was executed twice, firstly on the as-quenched and then on the as-aged alloy. Chen et al. [29] studied the effects of CTs on an unspecified aerospace aluminium alloy, obtaining opposite results. Precisely, they measured an increase in the hardness which was not accompanied by an improvement of the tensile properties. No improvement was found in fatigue strength. Conversely, K. Mohan [38] investigated the response of a 7075-T6 aluminium alloy to a shallow cryogenic treatment (SCT) at $-80\text{ }^{\circ}\text{C}$ for 72 h, and reported a significant improvement in fatigue resistance (+65%) and a slighter increase in UTS. Recent studies suggested the formation of hard secondary phases [32, 33], grain-size effects [34] and the generation of dislocations [35]. Baldissera et al. [30] presented a review of CTs of several alloys resulting in a finer grain size and optimum dispersion of secondary phases. The study of Cabezea et al. [8] on 2xxx aluminum alloys showed that the CT increases the secondary incoherent nanoparticles in intergranular regions, and this slight precipitation did not produce any modification of the mechanical properties but an improvement in stress-corrosion cracking resistance. Bouzada et al. [33] studied cryogenic treatments at 98 K on aerospace AA7075 T6 alloy and demonstrate by TEM that the nature of the precipitates do not have any changes after DCTs. The DCTs effect is to change the distribution of the precipitates. For this reason, the authors suggest that this can strongly affect only the SCC behaviour of the alloy.

The research conducted by Li et al. [38] showed that the exposure time at cryogenic temperatures can affect the mechanical properties of an Al–Zn–Mg–Cu alloy, even if the treatment time does not affect the mechanical resistance significantly. Dobbins and Barron [45, 46] studied the effect of the exposure time and temperature on the final material properties. Lulay et al. [25] studied the response of a 7075 aluminum alloy after cryogenic treatment of 2 and 48 h, but no significant changes were observed in the mechanical resistance. The research conducted by Li et al. [38] showed that the exposure time at cryogenic temperatures can significantly affect the mechanical properties of an Al–Zn–Mg–Cu alloy, even if the mechanical strength is not linearly related to the treatment time.

Table 1 Nominal chemical composition in wt. % of the 7050 aluminum alloy

% Zn	% Mg	% Cu	% Zr	% Al
6.21	2.10	2.19	0.10	Bal

**Fig. 1** LOM observations of the 7050 AA, T76 temper for the L-ST and LT-ST planes

The technical literature is much debated on the topic and the reported data are often contradictory, indicating trifling improvement. The aim of this investigation is to clarify the influence of different heat treatment conditions on the response to DCTs of a high resistance 7050 AA, in terms of mechanical and intergranular corrosion behaviour.

Finally, the paper aims to clarify the precipitates distribution induced by DCTs and justify the variation in corrosion susceptibility in high-performance 7xxx aluminum alloys after DCTs.

2 Materials and methods

The present experimental investigation is focused on AA7050 aluminum alloy. The material was delivered as 100 mm thick plates in the T7451 temper, and the nominal chemical composition is reported in Table 1.

The metallographic analysis was carried out along the three rolling directions. Example of the image are shown in Fig. 1 for T76 condition.

The deep cryogenics treatment (DCT) was performed at $-196\text{ }^{\circ}\text{C}$ by dipping the specimens in liquid nitrogen. The heating back to room temperature was carried out slowly by means of an insulated box. Temperature was measured by a thermocouple in the box. The ambient temperature was reached in two hours, which is a value in agreement with the technical literature [33]. To study the influence of low temperature on corrosion and mechanical performance, laboratory heat treatments were carried out to obtain T76 temper samples with and without CTs. The investigated conditions are described in Table 2. The influence of soaking time was investigated by hardness tests, and 72 h of soaking was selected for mechanical and corrosion tests.

To determine the mechanical resistance of the investigated conditions, tensile tests were carried out on specimens from the long transverse (LT) direction using an Instron 4507 H universal machine, according to standard ISO 6892-1:2016 [47].

The tensile specimen geometry is shown in Fig. 2. The size of specimens machined along the short-transverse direction was reduced because of the thickness of the as-supplied material. Tests were carried out with 2 mm/min strain rate, and six samples per each conditions were tested.

Intergranular corrosion tests were performed on prismatic specimens with dimensions equal to 25 mm \times 25 mm \times 20 mm. According to standard ASTM G110-92 [44], they were immersed for 24 h in a solution

Table 2 Details of the laboratory heat-treating procedures

Id. code	Treatment procedure
T7451	As-delivered
T7451C	As-delivered, 72 h cryogenic soaking
T76	Solution treatment at 477 °C, aging at 121 °C 4.5 h + 166 °C 14 h
T76C	Solution treatment at 477 °C, aging at 121 °C 4.5 h + 166 °C 14 h, 72 h cryogenic soaking
T76SC	Solution treatment at 477 °C, 72 h cryogenic soaking, aging at 121 °C 4.5 h + 166 °C 14 h

The solution treatment and aging temperatures satisfy the ASTM B918/B918 M–17a standard [1]

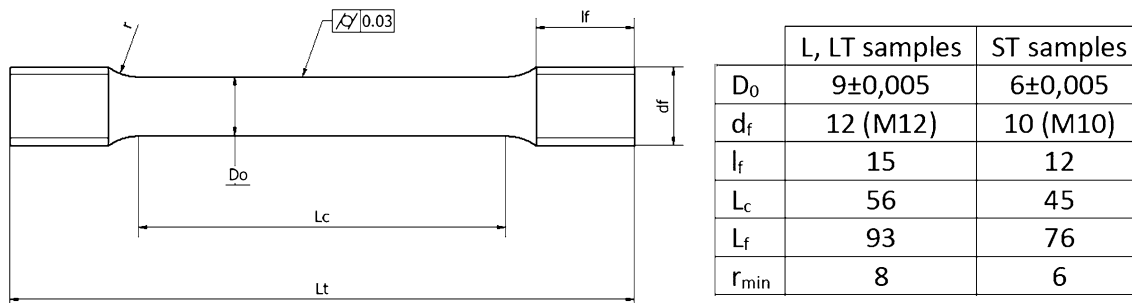


Fig. 2 Drawing and dimensions of the tensile specimens

Fig. 3 Procedure for the analysis of the corroded profiles: **a** sample immersed in the testing solution; **b** cut along the L-ST plane; **c** observed corroded profile

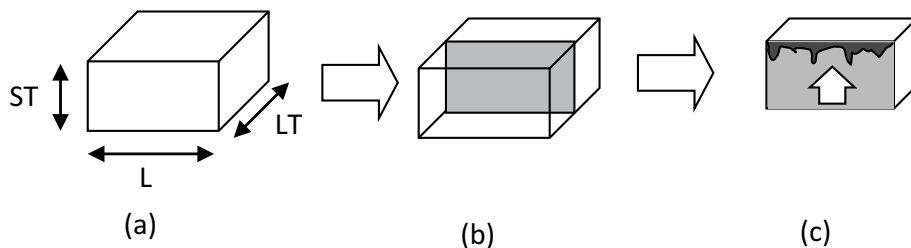
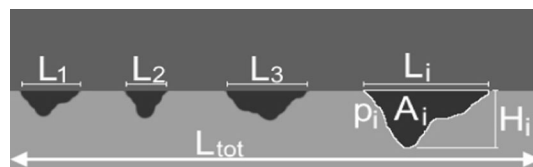


Fig. 4 Image analysis of a corrosion pit



composed of NaCl (57 g) and H₂O₂ (10 mL) diluted to 1 L with reagent water. All the plate surfaces (L-LT, L-ST, LT-ST–L is the longitudinal direction, LT is the long transverse direction and ST is the short transverse direction) were exposed to the corrosive environment after grinding with 120-grit paper. Figure 3 shows a scheme of the sample preparation for microscopic observation after corrosion tests.

The evaluation of the corrosive attack was performed by image analysis according to the procedure described in literature [45]. Referring to Fig. 4, each pit has been described by measuring its depth, width and roundness, which is defined according to Eq. (1).

$$R_i^* = R_i \frac{H_i}{L_i} \quad (1)$$

$$R_i = \frac{P_i^2}{4\pi S_i} \quad (2)$$

where R_i^* is the modified roundness, R_i is the standard roundness defined by Eq. (2), P_i is the perimeter of the i -th pit and S_i is the area of the i -th pit. Since the mechanical properties of the alloy can be decreased by the presence of multiple corrosion pits, a parameter representative of the surface condition is important to be defined. This value, called C_S and reported in Eq. (3), is defined as the ratio between the total length of the defects and the total length of the original profile.

$$C_S = 100 \frac{\sum_i L_i}{L_{tot}} \quad (3)$$

where L_i is the length of the i -th corrosion pit and L_{tot} is the total length of the original profile (with no corrosion pits). Finally, Eq. (4) provides a parameter representative of the whole surface damage in the presence of corrosion:

$$R_C = C_S R^* \quad (4)$$

where R^* is the average modified roundness. The corrosion resistance increases when R_C decreases.

3 Experimental results and discussion

The influence of soaking time at -196°C was initially investigated by hardness tests (HBW 2.5/62.5) on T76 specimens. Varying the initial heat-treating condition, Fig. 5 shows the influence of cryogenic treatment on hardness as a function of time.

The experimental data showed no appreciable difference among the tested conditions. In the technical literature, the influence of soaking time is debated. Dobbins and Barron [45, 46] claim that the exposure time at cryogenic temperature directly affects the final material properties. Lulay et al. [25] studied the response of a 7075 aluminum alloy after cryogenic treatment of 2 and 48 h, but no significant changes were observed in the mechanical resistance. The research conducted by Li et al. [38] showed that the exposure time at cryogenic temperatures can significantly affect the mechanical properties of an Al–Zn–Mg–Cu alloy, even if the mechanical strength is not linearly related to the treatment time. In the present paper, the authors decided to perform DCTs at -196°C with 72 h soaking, which is the maximum investigated time. Figure 6 shows the results of tensile tests for LT direction.

The obtained results show no or a very limited influence of the cryogenic treatment. This behavior was already observed by other authors [45, 46] on a 7075 aluminum alloy, which has a chemical composition similar to that of 7050 aluminum alloys.

Fig. 5 Influence of soaking time at -196°C on hardness

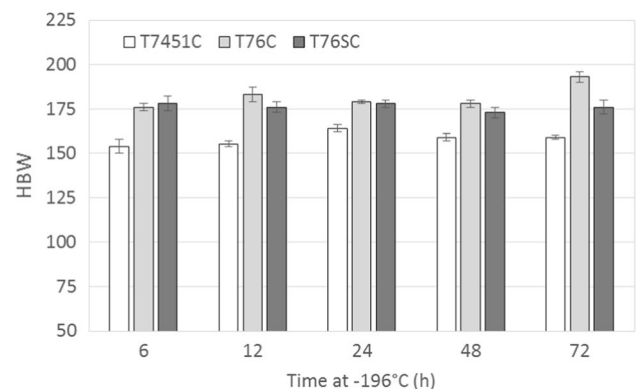
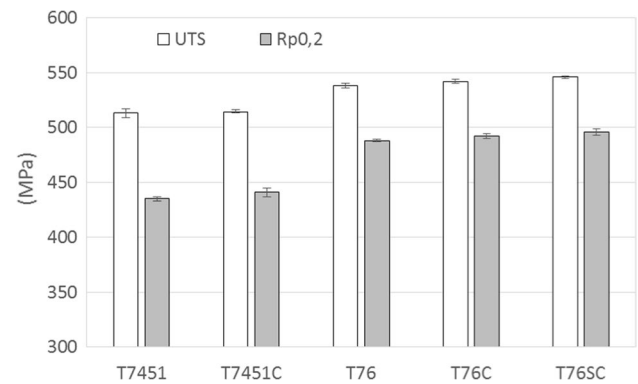


Fig. 6 Ultimate tensile strength (UTS) and yield strength (Rp0.2) in the investigated conditions, LT direction



The tensile test results were represented with true stress-true strain approach for analyzing the plastic behavior of the alloys. For a better understanding, the plastic curves were described with Hollomon equation reported in Eq. (5)

$$\sigma^* = K \varepsilon^{*n} \quad (5)$$

where, σ^* is the true stress; ε^* is true strain; K , n are constants specific for the material.

Table 3 shows the Hollomon parameters calculated from the true stress-true strain curve, Agt i.e. the total elongation at maximum force and the modulus of toughness MT (specific energy per unit volume absorbed by the samples before rupture) for each examined condition. The results show that the effects of DCTs on the plastic behavior can be considered negligible, while they seem to have some effect in decreasing the Agt and the modulus of toughness.

After the mechanical tests, the intergranular corrosion resistance was studied. All the rolling planes (L-LT, L-ST and LT-ST) were exposed to the test solution. Figure 7 shows some examples of corrosion pits developed from the L-ST plane.

The images acquired after corrosion were investigated by quantitative analysis. Figure 8 shows a comparison among the investigated conditions as a function of the parameter evaluated in all the rolling directions.

The obtained results show that the value is influenced by the CT. In particular, in the T76 temper, its value decreases especially in the presence of cryogenic treatment carried out between solubilization and aging (T76SC condition). This observation is confirmed by the average values shown in Fig. 9.

For a better understanding of the metallurgical mechanisms involved, the pit morphology was investigated by calculating the modified roundness, in all the experimental conditions. The analysis was concentrated on L-ST plane, which is found to be the most critical rolling direction. Figures 10 and 11 show the modified roundness values as a function of the area for each pit in all the experimental conditions. The obtained results show that the pit morphology is similar in all the investigated conditions. However, the main difference is related to the number of pits and, in the presence of cryogenic treatment, this value decreases significantly, as shown in Fig. 12. In conclusion, the metallurgical quantitative analysis of the corroded samples shows that the cryogenic treatment is able to produce a decrease in the pit number, while it has a negligible influence on the pit morphology.

4 Discussion

From the technical literature, it is well known that the precipitation sequence of the 7000 series Al alloys can be summarized as: solid solution–GP zone–metastable η' —stable η (MgZn₂). For the peak aged (T6) 7000 series aluminum alloys, the η' phase is the main precipitate; however, for the over aged temper (T7 ×) the η phase is the main precipitate.

Table 3 Tensile test parameters for the different examined conditions

	T451	T451C	T76	T76C	T76SC
K	716 ± 44	734 ± 20	725 ± 35	733 ± 18	712 ± 29
n	0.10	0.10	0.08	0.09	0.08
Agt [%]	8.1 ± 1	7.6 ± 1.5	9.1 ± 2.0	8.9 ± 1.3	8.5 ± 1.5
MT [J/mm ³]	63.2 ± 3.5	57.3 ± 2.8	80.7 ± 3.2	75.1 ± 2.4	67.8 ± 2.8

Fig. 7 Corrosion pits observed in the T7451C (a), T76 (b), T76C (c) and T76CS (d) specimens

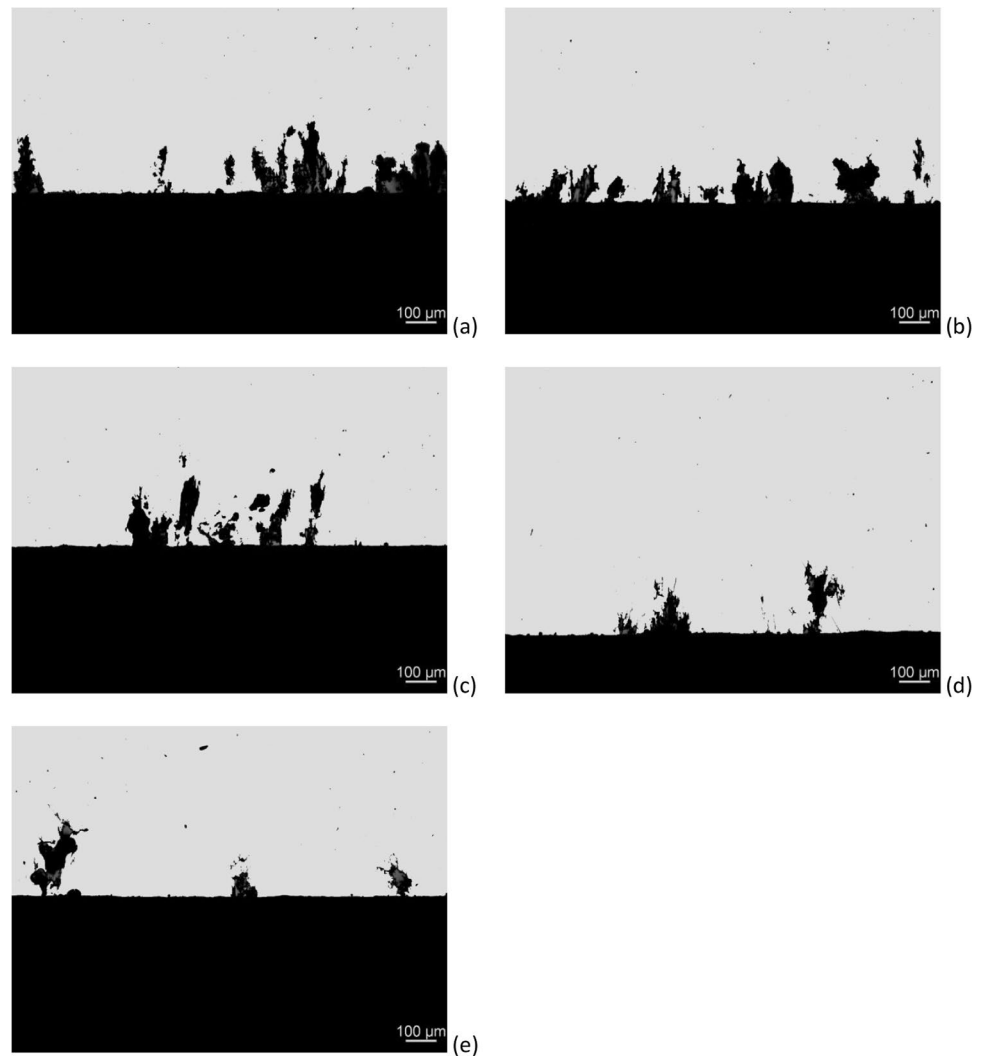
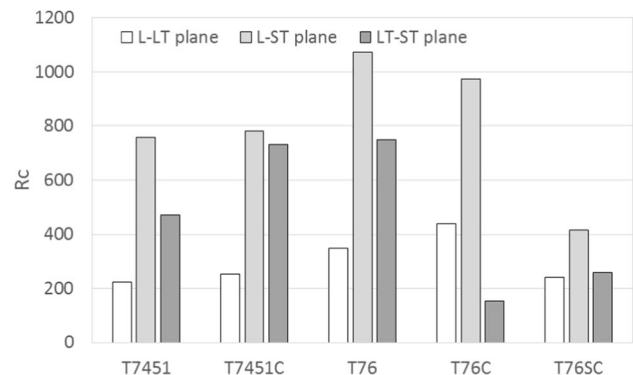


Fig. 8 R_c parameter in all the rolling directions in each heat-treating condition after corrosion test



Bouzada [33] already showed that CTS do not change the nature of the precipitates in 7XXX metal matrix. This confirms the trifling influence of the DCT on the mechanical strength and on the plastic behavior of the material, demonstrated in this investigation. The toughness parameters calculated from tensile curve seem to be slightly influenced by DCTs.

Intergranular corrosion is caused by potential differences between grain boundary regions and the adjacent grain cores and it develops because of some heterogeneity in the grain boundaries structure [1]. Intergranular corrosion resistance is affected by the distribution of the precipitates near the grain boundaries. That's why for a better understanding of the metallurgical phenomena involved, the corroded T76, T76C and T76SC samples were investigated

Fig. 9 Average values for T76, T76C and T76SC tempers

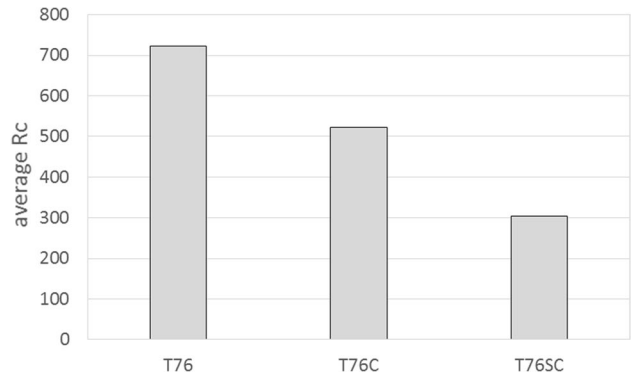


Fig. 10 Comparison among the modified roundness values in T7451 and T7451C tempers as a function of the pit area

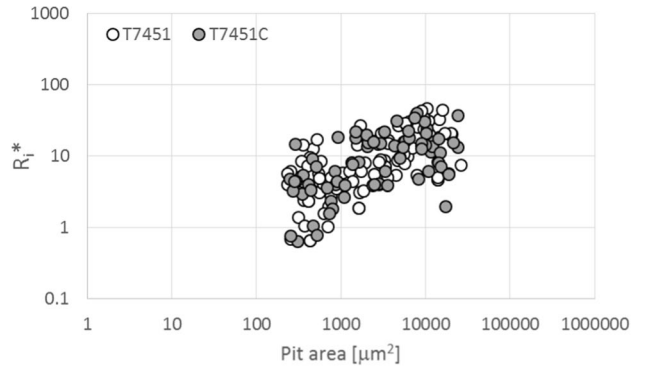


Fig. 11 Comparison among the modified roundness values in T76, T76C and T76SC tempers as a function of the pit area

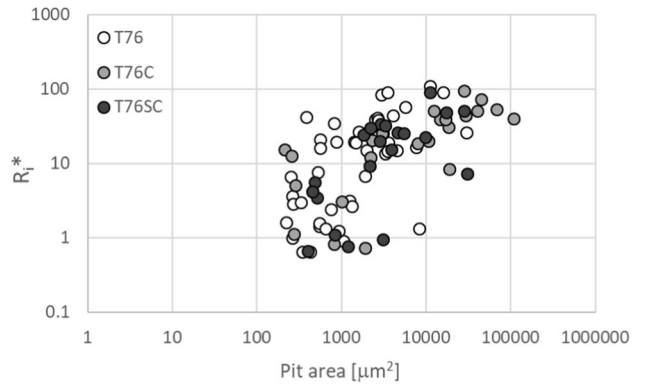
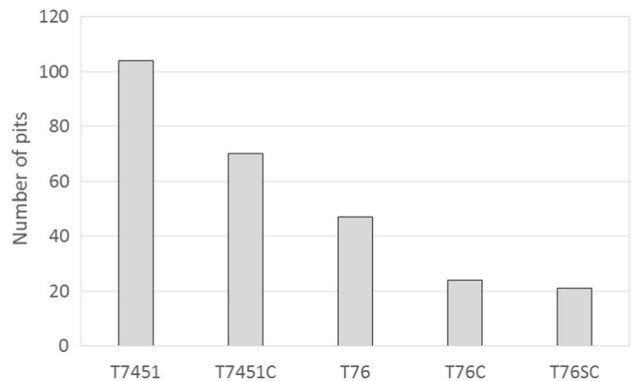


Fig. 12 Comparison among the number of pits in all the heat-treating conditions



by scanning electron microscopy (Zeiss Sigma 500 SEM), and the precipitate distribution at the grain boundaries was observed. Images at very high magnifications by SEM were acquired and compared to analyze the precipitates distribution in the metallic matrix. The images are shown in Figs. 13, 14, 15.

The comparison among the previous images shows a significant difference in the precipitates distribution. The cryogenic treatment produces a finer and more homogeneous precipitation of secondary phases in the whole grain. This phenomenon can be considered as responsible to enhance the corrosion susceptibility of aluminum alloys [1–5], as also recently documented by Bouzada et al. [41]. The homogenous precipitates distribution induces a lower electrochemical potential difference among the grain boundaries and the center-grain [41]. This behavior generates a

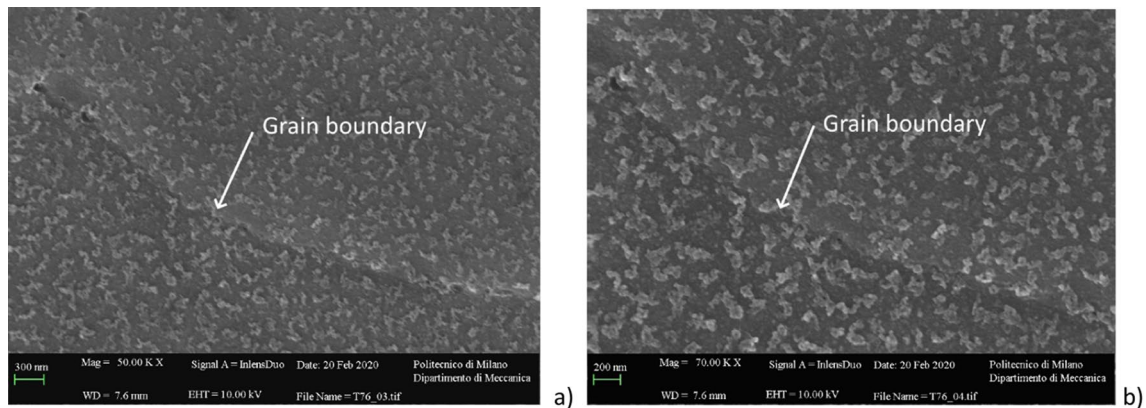


Fig. 13 Precipitate distribution at the grain boundaries—T76 temper. **b** is the magnification of **a**

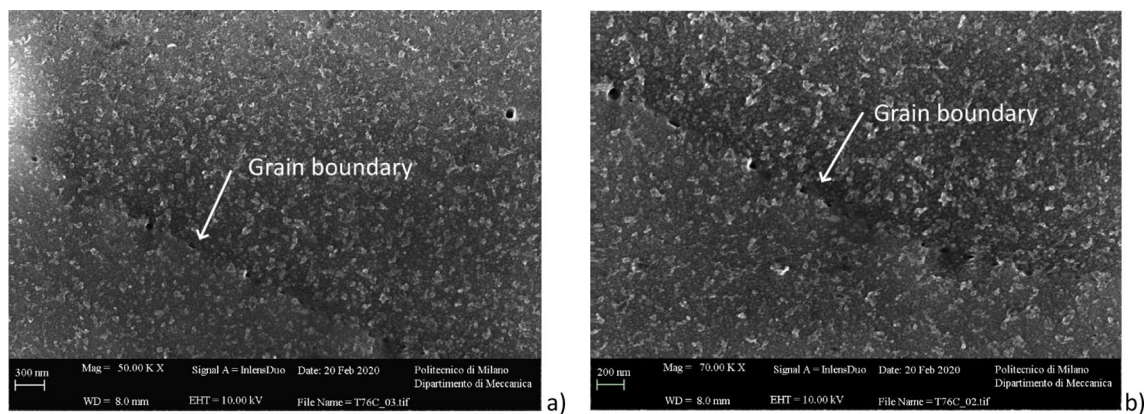


Fig. 14 Precipitate distribution at the grain boundaries—T76C temper. **b** is the magnification of **a**

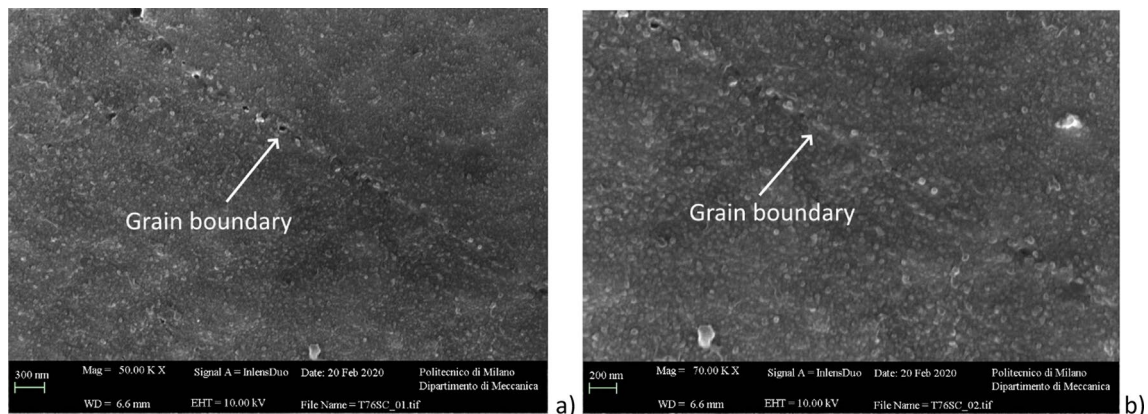


Fig. 15 Precipitate distribution at the grain boundaries—T76SC temper. **b** is the magnification of **a**

higher corrosion resistance of grain boundaries, and finally, a higher intergranular-corrosion resistance of the whole material.

5 Conclusions

In the present paper, the influence of DCT on a high performance 7050 AA was investigated. Two treatment tempers were considered: T7451, the as-delivered, and T76, obtained by laboratory solubilization and aging. Cryogenic soaking at $-196\text{ }^{\circ}\text{C}$ was carried out on both the as-delivered sample and the T76 temper. In the latter, cryogenic treatment was performed both after aging and between solution and aging. The corrosion resistance was found to be improved, especially in the T76 temper. Microscopic observations revealed a different precipitate distribution at the grain boundaries after cryogenic treatment. The best corrosion resistance was obtained when soaking at $-196\text{ }^{\circ}\text{C}$ was carried out between solution and aging. Tensile strengths are not significantly influenced by such different precipitate distributions, while toughness parameters seem to be slightly decreased by DCTs. Future development of this project will be focused on stress-corrosion cracking tests to confirm the obtained results. Moreover, different soakings at $-196\text{ }^{\circ}\text{C}$ will be considered to study the influence of the exposure time on the corrosion susceptibility and toughness parameters.

Author contributions DP and RG performed the experimental mechanical tests. AC performed the LOM analysis BR performed the SEM images and prepared the manuscript.

Funding The authors did not receive support from any organization for the submitted work.

Data availability The datasets generated during and/or analysed during the current study are available from the corresponding author on reasonable request.

Declarations

Competing interests All authors certify that they have no affiliations with or involvement in any organization or entity with any financial or non-financial interest in the subject matter or materials discussed in this manuscript. The authors declare no competing interests.

Open Access This article is licensed under a Creative Commons Attribution 4.0 International License, which permits use, sharing, adaptation, distribution and reproduction in any medium or format, as long as you give appropriate credit to the original author(s) and the source, provide a link to the Creative Commons licence, and indicate if changes were made. The images or other third party material in this article are included in the article's Creative Commons licence, unless indicated otherwise in a credit line to the material. If material is not included in the article's Creative Commons licence and your intended use is not permitted by statutory regulation or exceeds the permitted use, you will need to obtain permission directly from the copyright holder. To view a copy of this licence, visit <http://creativecommons.org/licenses/by/4.0/>.

References

1. ASTM 918/B918M–09. Standard practice for heat treatment of wrought aluminum alloys. ASTM Int. 2009.
2. George E, MacKenzie DS. Handbook of aluminum, volume 7, physical metallurgy and processes. New York: Marcel Dekker Inc; 2003.
3. Anderson K, Weritz J, Kaufman,. Aluminum science and technology ASM handbook, vol. 2A. Almere: ASM International; 2018.
4. Chinella JF, Guo Z. Computational Thermodynamics Characterization of 7075, 7039, and 7020 Aluminum Alloys Using JMatPro. Adelphi: U>S. Army Research Laboratory; 2011.
5. Li J, Li F, Ma X, Li J, Liang S. Effect of grain boundary characteristic on intergranular corrosion and mechanical properties of severely sheared Al-Zn-Mg-Cu alloy. *Mater Sci Eng A*. 2018;732:53–62.
6. Franco Steier V, Ashiuchi ES, Reißig L, Araújo JA. Effect of a deep cryogenic treatment on wear and microstructure of a 6101 aluminum alloy. *Adv Mater Sci Eng*. 2016. <https://doi.org/10.1155/2016/1582490>.
7. Wang JJ, Xue XD, Yang ZQ, Zhang H, Zhou Y. Effect of cryogenic treatments on mechanical properties of 2A11 aluminum alloy. *Adv Mater Res*. 2011;146–147:1646–50.
8. Cabeza M, Feijoo I, Merino P, Trillo S. Effect of the deep cryogenic treatment on the stress corrosion cracking behaviour of AA 2017–T4 aluminium alloy. *Mater Corros*. 2016;67(5):504.
9. Schiradelly R, Diekman FJ. A research review on deep cryogenic treatment of steels. *Heat Treat Prog*. 2001;8:43.
10. Kalia S. Cryogenic processing: a study of materials at low temperatures. *J Low Temp Phys*. 2010;158:934.
11. Das D, Dutta AK, Ray KK. *Mater. Sci Eng A*. 2010;527:2182.
12. Baldissera P, Delprete C. Deep cryogenic treatment: a bibliographic review. *Open Mech Eng J*. 2008;2:1.
13. Reitz W, Pendray J. Cryoprocessing of materials: a review of current status. *Mater Manuf Processes*. 2001;16(6):829–40.

14. Chitrang AD, Kulkarni VA, Sonar K. A Review on the effect of cryogenic treatment on metals. *Int Res J Eng Technol.* 2017;4(7).
15. Kalia S, Processing C. A study of materials at low temperatures. *J Low Temp Phys.* 2010;158:934–45.
16. da Silva F, Franco S, Machado A, Ezugwu E, Souza AM. Metallurgical principles of cryogenically treated tool steels—a review on the current state of science. *Wear.* 2006;261:674.
17. Singandhupe RB, Sethi RR. Cryogenic tool treatment. *Imp J Interdiscip Res.* 2016;2(9):300.
18. Yang H, Jun W, Bao-Luo S, Hao-Huai L, Sheng-Ji G. Effects of deep cryogenic treatment on wear resistance and structure of GB 35CrMoV steel. *Wear.* 2006;261:1150.
19. Bensely A, Senthilkumar D, Lal DM, Nagarajan G, Rajadurai A. Effect of cryogenic treatment on tensile behavior of case carburized steel-815M17. *Mater Charact.* 2007;58:485–91.
20. Baldissera P. Deep cryogenic treatment of AISI, 302 stainless steel: part i—hardness and tensile properties. *Mater Des.* 2010;31:4725–30.
21. Araghchia M, Mansouria H, Vafaiea R, Yina G. A novel cryogenic treatment for reduction of residual stresses in 2024 aluminum alloy. *Mater Sci Eng A.* 2017;689:48–52.
22. Pavan KM, Sachin LS, Mayur S, Chandrashekar A, Ajaykumar BS. Effect of cryogenic treatment on the mechanical and microstructural properties of Aluminum alloys—a brief study. *Int J Mech Prod Eng.* 2014;2(5):95.
23. Chen D, Li W. Cryogenic treatment of Al and Al alloys. *Chin J Nonferrous Met.* 2000;10(6):891.
24. Liu Y, Shao S, Xu CS, Zeng XS, Yang XJ. Effect of cryogenic treatment on the microstructure and mechanical properties of Mg–1.5Zn–0.15Gd magnesium alloy. *Mater Sci Eng A.* 2013;588:76.
25. Asl KM, Tari A, Khomamizadeh F. Effect of deep cryogenic treatment on microstructure, creep and wear behaviors of AZ91 magnesium alloy. *Mater Sci Eng A.* 2009;523:27.
26. Gu K, Zhang H, Zhao B, Wang J, Zhou Y, Zhou Y. Effect of cryogenic treatment and aging treatment on the tensile properties and microstructure of Ti–6Al–4V alloy. *Mater Sci Eng A.* 2013;584:170.
27. Lulay KE, Khan K, Chaaya D. The effect of cryogenic treatments on 7075 aluminum alloy. *J Mater Eng Perform.* 2002;11:479.
28. Wang QC, Wang LT, Peng W. Thermal stress relief in 7050 aluminum forgings by uphill quenching. *Mater Sci Forum.* 2005;490–491:97.
29. Chen P, Malone T, Bond R, Torres P. Effects of cryogenic treatment on the residual stress and mechanical properties of an aerospace aluminum alloy. In: *Proc 4th Conf Aerosp Mater Process Environ Technol.* 2001.
30. Baldissera P, Delprete C. Deep cryogenic treatment: a bibliographic review. *Open Mech Eng J.* 2008;2:1–11.
31. Steier VF, Ashiuchi ES, Reißig L, Araújo JA. Effect of a deep cryogenic treatment on wear and microstructure of a 6101 aluminum alloy. *Adv Mater Sci Eng.* 2016. <https://doi.org/10.1155/2016/1582490>.
32. Li G, Wang H, Cai Y, Yuan X. Behavior of $\beta(\text{Mg}_{17}\text{Al}_{12})$ phases in mg-al alloy subject to cycling cryogenic treatment. *Key Eng Mater.* 2014;575–576:390–3.
33. Karabay S, Yilmaz M, Zeren M. Investigation of extrusion ratio effect on mechanical behaviour of extruded alloy AA-6101 from the billets homogenised-rapid quenched and as-cast conditions. *J Mater Process Technol.* 2005;160(2):138–47.
34. Jiang X-Q, Li N, He H, Zhang X-J, Li C-C, Yang H. Effect of cryogenic treatment on mechanical properties and microstructures of 3102 Al-alloy. *Mater Sci Forum.* 2007;546–549(2):845–8.
35. Gu K, Wang J, Zhou Y. Effect of cryogenic treatment on wear resistance of Ti-6Al-4V alloy for biomedical applications. *J Mech Behav Biomed Mater.* 2014;30:131–9.
36. Desai RS, Joshi AG, Kumar S. Study on influence of cryogenic treatment on mechanical properties of AlSi10Mg alloy. *Int J Res Eng Technol.* 2016;5:53.
37. Jiangm XQ, Li N, He H, Zhan XJ. Effect of cryogenic treatment on the fatigue crack propagation behavior of 7075 aluminum alloy. *Mater Sci Forum.* 2007;546:845.
38. Mohan K, Suresh JA, Ramu P, Jayaganthan R. Microstructure and mechanical behavior of Al 7075–T6 subjected to shallow cryogenic treatment. *J Mater Eng Perform.* 2016;25(6):2185.
39. Zhang WD, Bai PK, Jing YA, Hong XU, Dang JZ, Du ZM. Tensile behavior of 3104 aluminum alloy processed by homogenization and cryogenic treatment. *Trans Nonferrous Met Soc China.* 2014;24:2453–8.
40. Li CM, Cheng NP, Chen ZQ, Guo N, Zeng SM. Deep-cryogenic-treatment-induced phase transformation in the Al-Zn-Mg-Cu alloy. *Int J Miner Metall Mater.* 2014;22:68.
41. Wang QC, Wang LT, Pen W. Thermal stress relief in 7050 aluminum forgings by uphill quenching. *Mater Sci Forum.* 2005;490–491:97–101.
42. Zhou J, Xu S, Huang S, Meng X, Sheng J, Zhang H, Li J, Sun Y, Boateng EA. Tensile properties and microstructures of a 2024–T351 aluminum alloy subjected to cryogenic treatment. *Metals.* 2016;6:279.
43. Bouzada F, Cabeza M, Merino P, Trillo S. Effect of deep cryogenic treatment on the microstructure of an aerospace aluminum alloy. *Adv Mater Res.* 2012;445:965–70.
44. Li CM, Cheng NP, Chen ZQ, Guo N, Zeng SM. Deep-cryogenic-treatment-induced phase transformation in the Al–Zn–Mg–Cu alloy. *Int J Miner Metall Mater.* 2015;22(1):68.
45. ASTM G110–92. Standard practice for evaluating intergranular corrosion resistance of heat treatable aluminum alloys by immersion in sodium chloride + hydrogen peroxide solution.
46. Gerosa R, Rivolta B, Derudi U. Influence of ageing on tensile and stress corrosion cracking behaviour of 7075 aluminium alloy plates. *Int J Microstruct Mater Prop.* 2010;5(1):15.
47. UNI EN ISO 6892-1:2016. Metallic materials—tensile testing—part 1: method of test at room temperature.